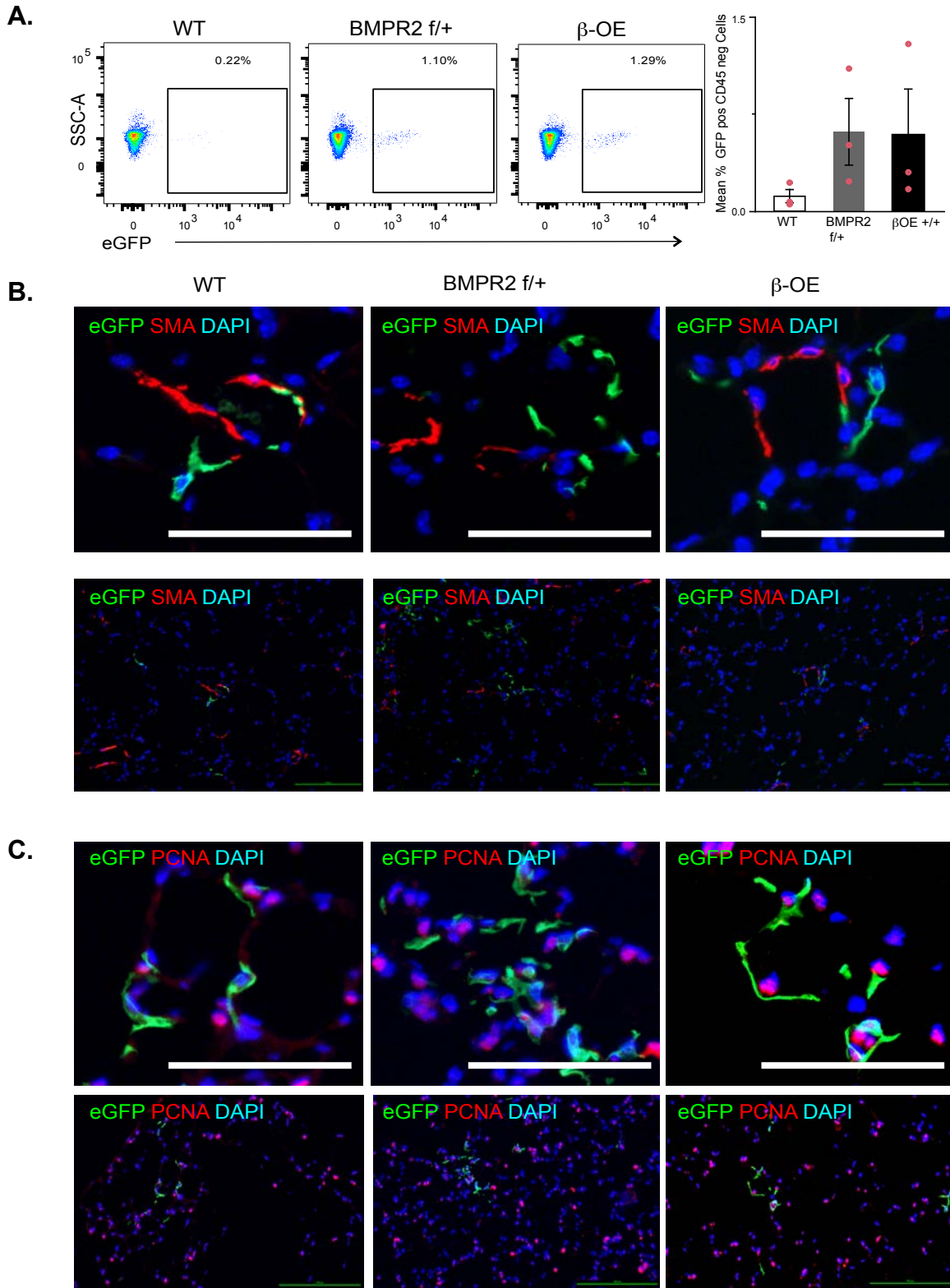
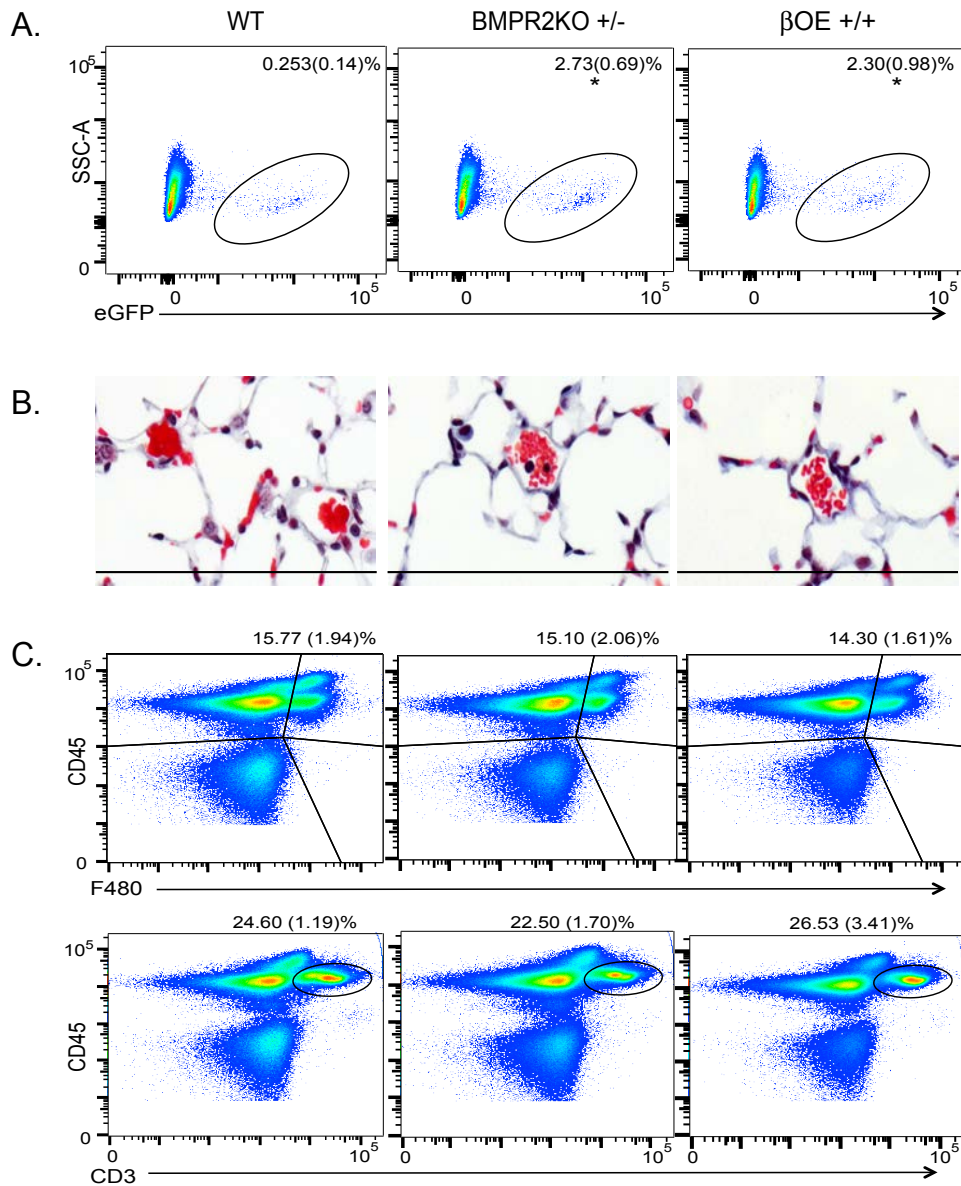


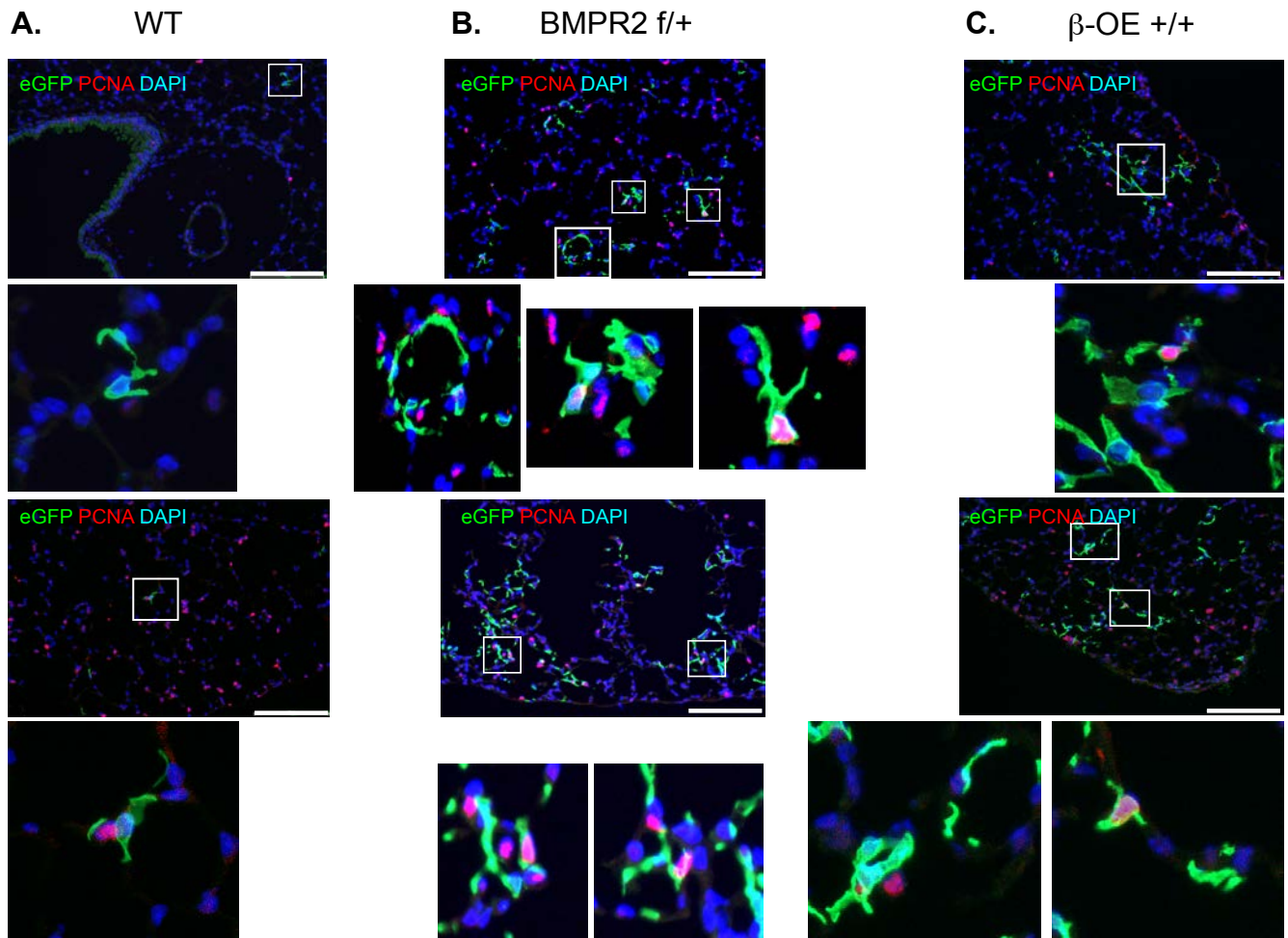
Supplemental Figures



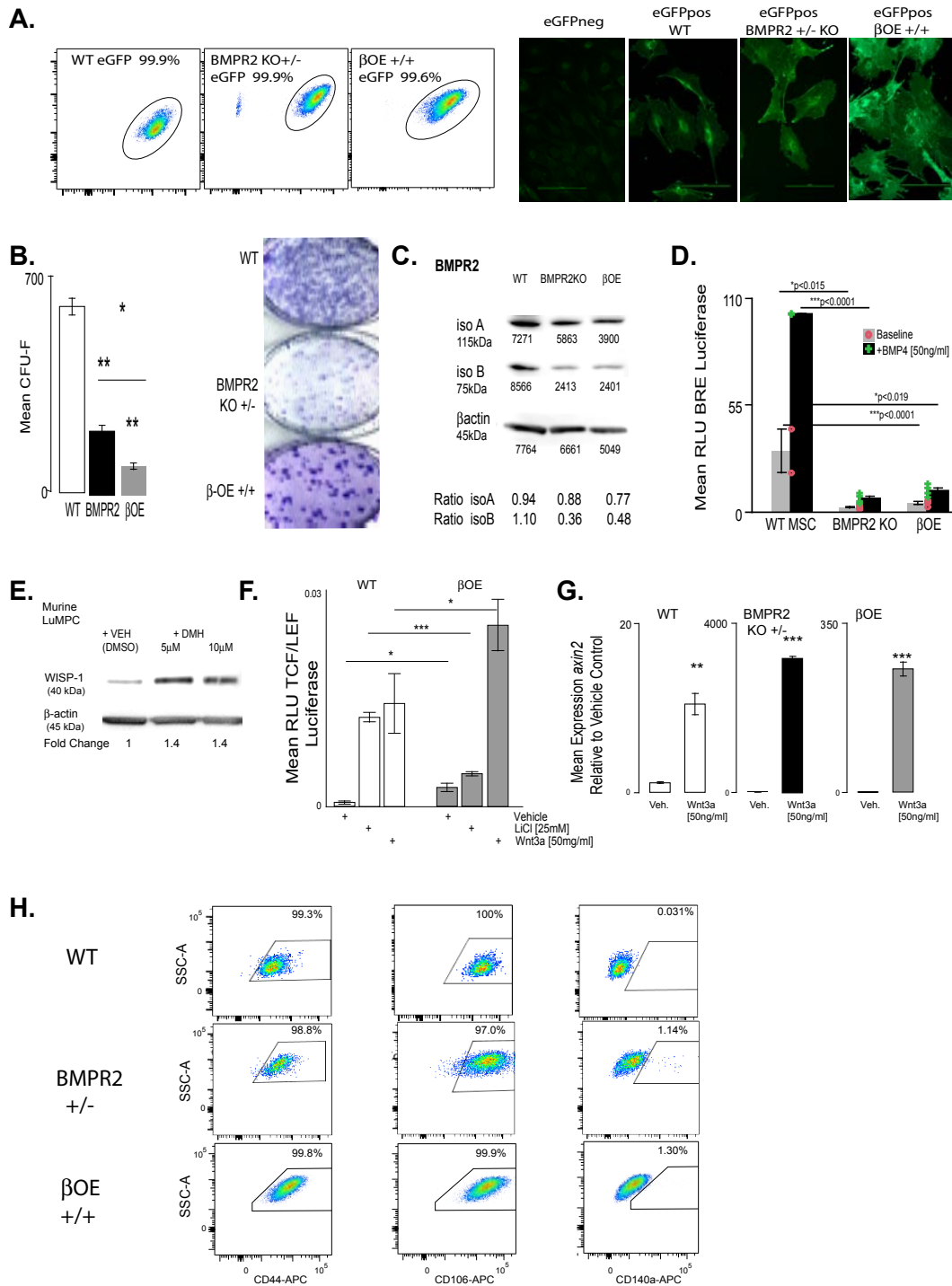
**Supplemental Figure 1. Related to Figure 1. Knockdown of BMPR2 or stabilization of  $\beta$ -catenin rapidly expands the murine  $Abcg2^{pos}$  lung mesenchymal progenitor pool by day2 post-induction.** WT,  $BMPR2^{f/+}$  and  $\beta$ OE mice were induced with intraperitoneal tamoxifen (0.5mg total). **A.** Two days following induction, eGFP labeling and enumeration of  $Abcg2^{pos}$  lung mesenchymal progenitors was confirmed by flow cytometry (n=3-6). **B&C.** Immunostaining was performed to detect  $Abcg2^{pos}$  mesenchymal progenitors and derived eGFP and SMA or PCNA expressing cells. Scale bars =50 mM (enlarged image) and 100mM. DAPI stained nuclei blue.



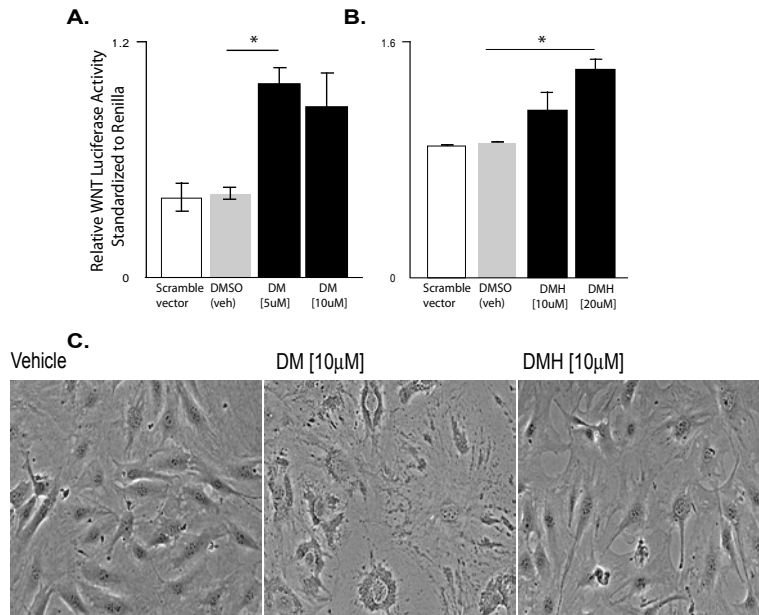
**Supplemental Figure 2. Related to Figure 1. Knockdown of BMPR2 or stabilization of  $\beta$ -catenin expands and maintains the murine Abcg2<sup>pos</sup> lung mesenchymal progenitor pool to 20 weeks.** **A.** Lineage labeling mice were induced with intra-peritoneal tamoxifen (0.5mg total). 18-20 weeks following induction, eGFP labeling and enumeration of Abcg2<sup>pos</sup> lung mesenchymal progenitors was confirmed by flow cytometry (n=3-6). Lung tissue was harvested and processed for histology. **B.** Trichrome staining was also performed. **C.** Flow cytometry was used to detect CD45/F480<sup>pos</sup> and CD45/CD3<sup>pos</sup> macrophages and T cells in single cell suspensions of lung tissue. Immunostaining was performed Scale bars =50, 75 or 100 $\mu$ m (B,D,C).



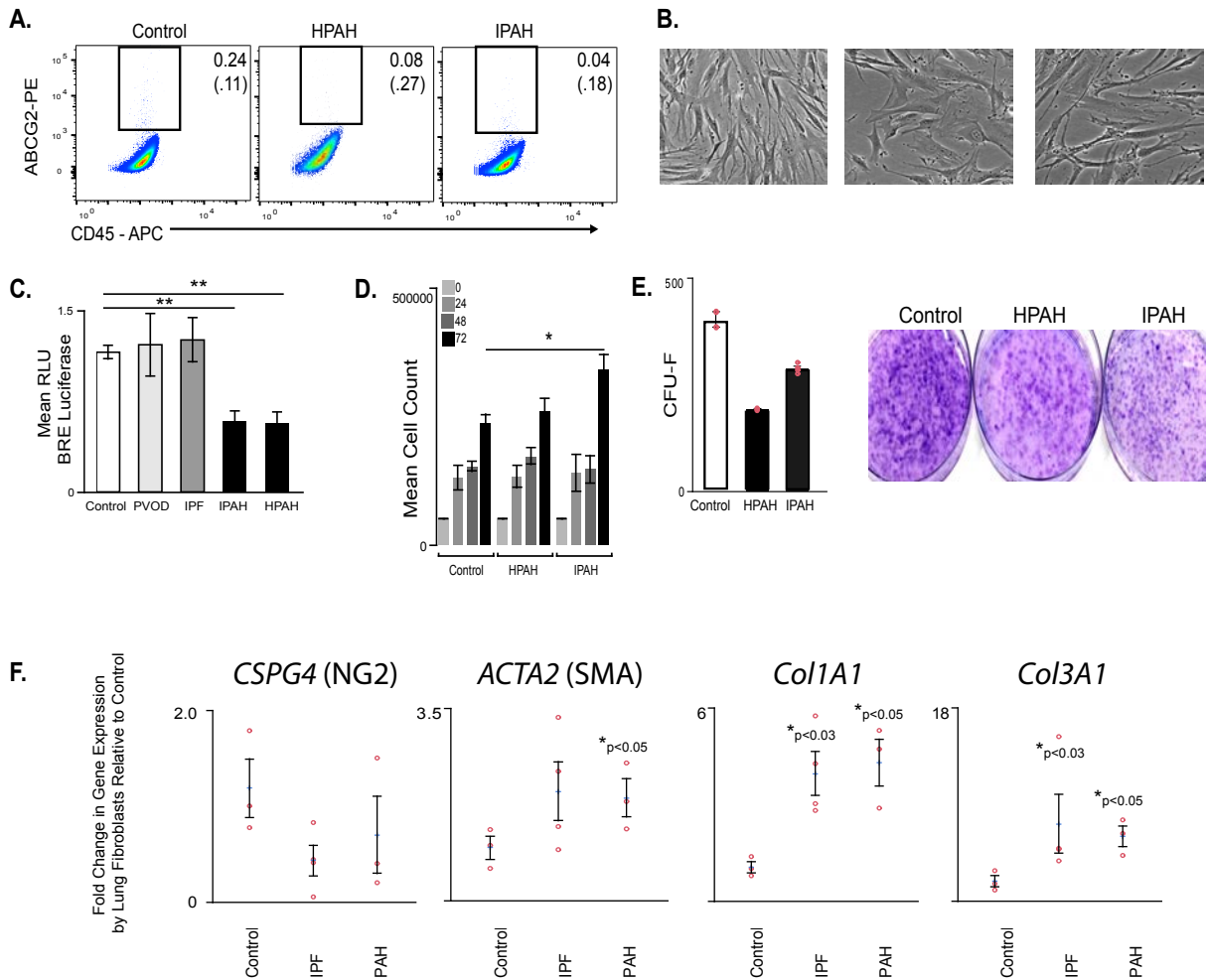
**Supplemental Figure 3. Related to Figure 1. Knockdown of BMPR2 or stabilization of  $\beta$ -catenin in *Abcg2*<sup>pos</sup> lung mesenchymal progenitors maintains the expanded MPC pool by day 14 post-induction.** A. WT B. *BMPR2*<sup>f/+</sup> and C.  $\beta$ OE mice were induced with intra-peritoneal tamoxifen (0.5mg total). Two weeks following induction Immunostaining was performed to detect eGFP<sup>pos</sup> *Abcg2*<sup>pos</sup> mesenchymal progenitors and derived cells and PCNA expressing cells. Scale bars =50 mM (enlarged image) and 100mM. DAPI stained nuclei blue.



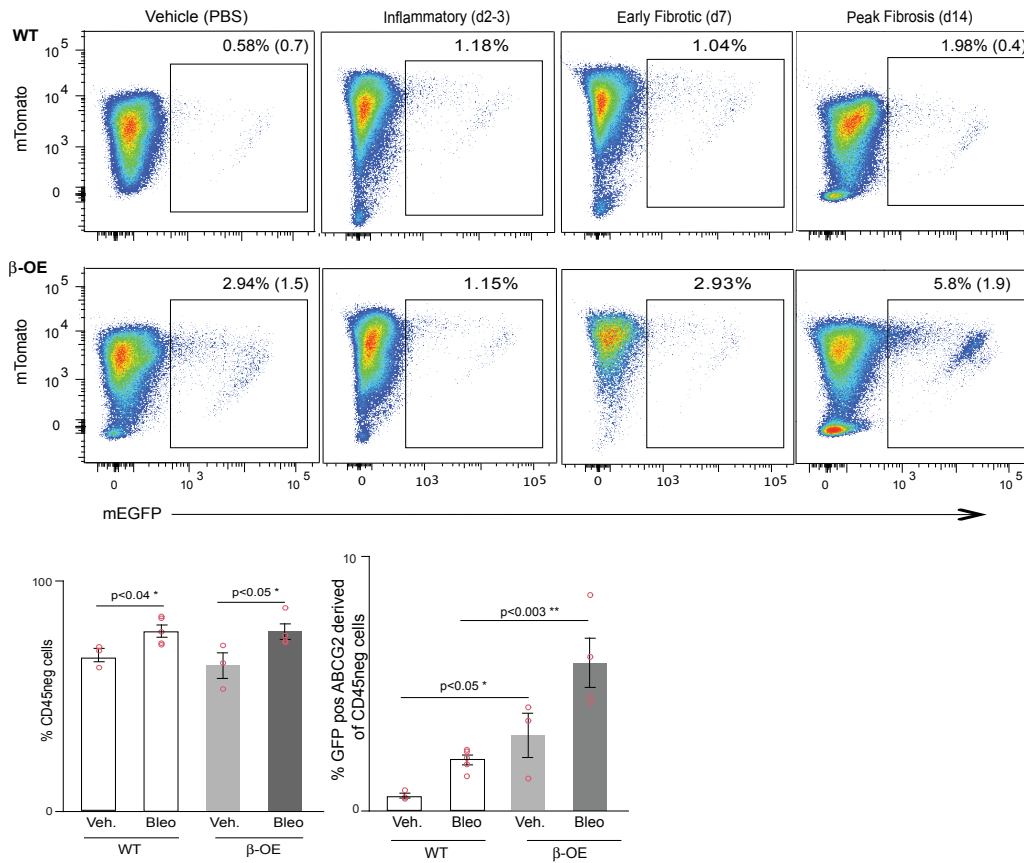
**Supplemental Figure 4. Related to Figures 1-5. Isolation and characterization of WT, BMPR2<sup>f/+</sup> and βOE Abcg2<sup>pos</sup> lung mesenchymal progenitors.** **A.** Lineage labeling mice were induced with intra-peritoneal tamoxifen (0.5mg total) and eGFP positive cells isolated by flow cytometry to establish cell lines. **B.** CFU-F assay was performed to quantitate clonogenic potential. **B.** Representative Giemsa stained CFU-F pictured. Data is presented as the mean (+/-SE). **C.** Western blot was performed to quantify relative levels of BMPR2 protein. **D.** BMPR2 signaling activity was evaluated using via luciferase assay. Luciferase activity was measured at 48 hours post transfection using a BRE BMPR2 reporter assay. BMP4 was used to stimulate BMPR2 signaling. **E.** Western blot was performed to quantify relative levels of WISP-1 protein following BMPR signaling inhibition in WT MPC. **F.** TCF/LEF luciferase analysis quantified the relative differences in canonical Wnt signaling in WT and βOE murine lung mesenchymal progenitors following stimulation with LiCL or Wnt3a. Data presented as the mean (+/-SE). **G.** qPCR was performed to detect axin2 expression in response to stimulation with Wnt3a ligand. **H.** Analysis of cell surface determinant by the primary ABCG2<sup>pos</sup> lung mesenchymal progenitors lines was performed using flow cytometry.



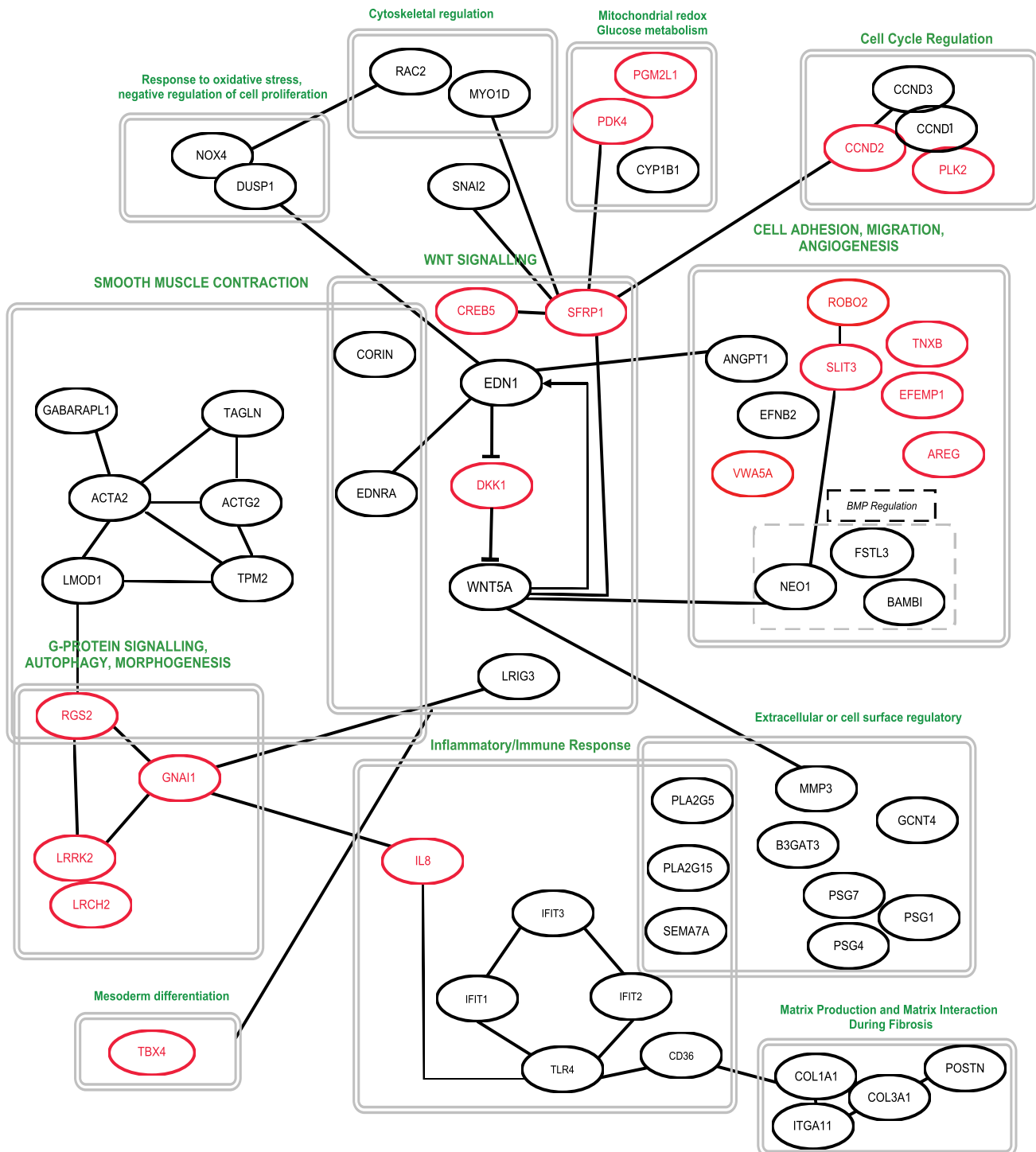
**Supplemental Figure 5. Related to Figure 2. Decreased BMPR2 signaling is associated with increased  $\beta$ -catenin/Wnt signaling activity in murine *Abcg22<sup>Pos</sup>* Lung mesenchymal progenitors.** BMPR2 signaling was decreased in WT lung mesenchymal progenitors using the small molecule inhibitors dorsomorphin (DM) and DMH1. DMH1 was presented in the manuscript because it is more specific for BMPR2. **A&B.** Luciferase activity was measured at 48 hours post transfection using a TCF/LEF canonical Wnt reporter assay. Data presented as the mean (+/-SE). **C.** Representative images of treated murine lung mesenchymal progenitors.



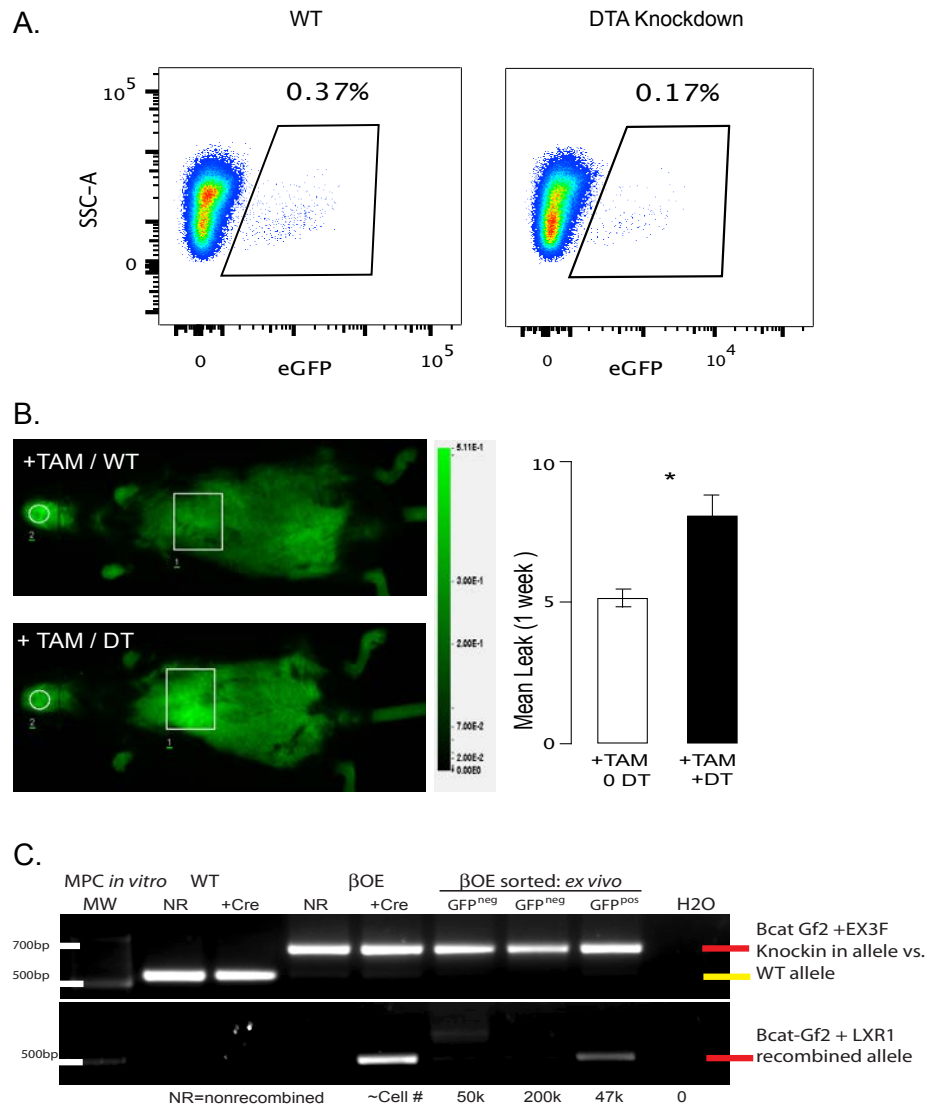
**Supplemental Figure 6. Related to Figures 2&5. Isolation and characterization of Human control and PAH ABCG2<sup>pos</sup> lung mesenchymal progenitors and FB.** **A.** Isolation of control, HPAH or IPAH ABCG2<sup>pos</sup> lung mesenchymal progenitors via surface expression of ABCG2 and lack of CD45. **B.** Representative bright field images of control, HPAH or IPAH ABCG2<sup>pos</sup> lung mesenchymal progenitors. **C.** BMP2 signaling activity was evaluated using via luciferase assay. Luciferase activity was measured at 48 hours post transfection using a BRE BMP2 reporter assay. **D.** Changes in control, HPAH or IPAH ABCG2<sup>pos</sup> lung mesenchymal progenitors cell number over a period of 0 to 72 hours were quantitated via trypan blue exclusion and automated cell counting. Results are presented as total numbers of viable cells per time point. **E.** Colony forming (CFU-F) assay was performed to detect differences in clonogenic potential between control, HPAH or IPAH ABCG2<sup>pos</sup> lung MPC. Representative Giemsa staining depicted. **F.** qPCR analyses of control, HPAH and IPAH (PAH) and IPF human lung FB was performed to quantitate relative levels of gene expression for pericyte lineage markers (*CSPG4*, *ACTA2*) as well as collagens 1 and 3 (*COL1A1*, *COL1A3*). Data presented as the mean (+/-SE).



**Supplemental Figure 7. Related to Figures 4&5. Enumeration of murine *Abcg2*<sup>pos</sup> lung mesenchymal progenitors in WT and βOE lungs following bleomycin injury.** Lineage labeled cells were analyzed by flow cytometry and quantitated increased numbers of eGFP expressing ABCG2<sup>pos</sup> lung MSC and derived cells following injury. Results are presented as % total numbers of viable cells per time point. Data presented as the mean (+/-SE).



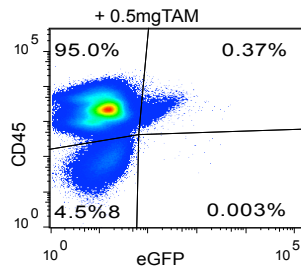
**Supplemental Figure 8. Related to Figure 5. Global gene expression analysis of ABCG2<sup>POS</sup> IPF Lung MPC links Wnt and BMP signaling to the maintenance of the MPC phenotype.** Functional association networks for genes that were differentially expressed in ABCG2<sup>poslung</sup> IPF MPC compared to control. Protein-protein interaction data from the STRING database and known gene function were utilized to draw the networks. Genes are represented by ovals containing gene symbols, with red ovals representing decreased and black ovals representing increased expression in ABCG2<sup>POS</sup> Lung IPF MPC. Lines connecting genes indicate direct physical interactions. Arrow-headed lines signify stimulatory and bar-headed lines signify inhibitory interactions. Functional gene categories are indicated by boxes, with appropriate captions.



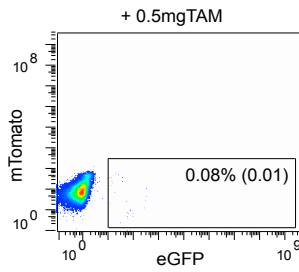
**Supplemental Figure 9. Related to Figures 1-5. Low Dose Tamoxifen induction of *Abcg2*<sup>CRE-ERT2</sup> MPC yields 50% Recombination Efficiency and Altered Microvascular stability *in vivo*.** WT, and DTA mice were induced with intra-peritoneal tamoxifen (0.5mg total). **A.** Two days following induction, eGFP labeling and enumeration of *Abcg2*<sup>pos</sup> lung mesenchymal progenitors was confirmed by flow cytometry (pooled n=3). **B.** One week following induction pulmonary vascular leak was quantitated. Representative images of mice obtained with the Pearl analyzer. A ratio was calculated for each animal comparing the intensity of dye in lung (square) to the baseline fluorescence in the nose (circle)- in bar graph (n=3-5). **C.** To demonstrate that recombination of floxed *ctnnb1* $\Delta$ ex3 is only detected in the eGFP<sup>pos</sup> fraction, we have performed genotyping PCR analysis on freshly isolated CD45<sup>neg</sup>/eGFP<sup>pos</sup>, putative MPC, and CD45<sup>neg</sup>/eGFP<sup>neg</sup>, 48 hours following induction (lanes 6-8) using sampled pooled from 3 mice or cell lines. As a positive control: Non-recombined WT and isolated BOE cells were transfected with a Cre recombinase expressing plasmid (lanes 2-5; pPGK-Cre-bpA was a gift from Klaus Rajewsky (Addgene, Cambridge, MA # 11543). The top gel uses primers to distinguish WT versus knock-in alleles (lanes 2&3 versus 4-8, respectively). The bottom gel uses a primer set that detects only recombined alleles.

ABCG2 Cre mT/eGFP

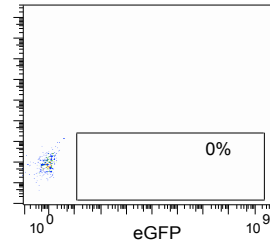
A. Donor WBM



B. Donor PBMC

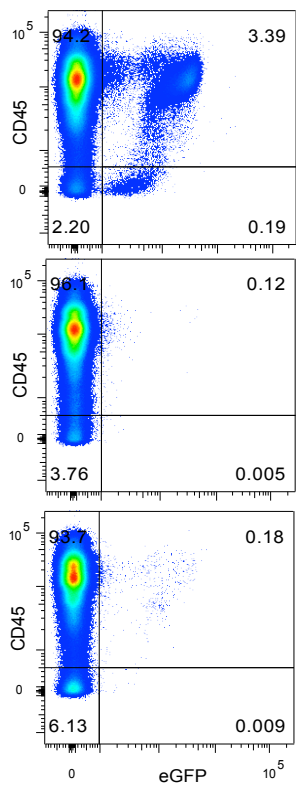


C. mTomato Recipient PBMC

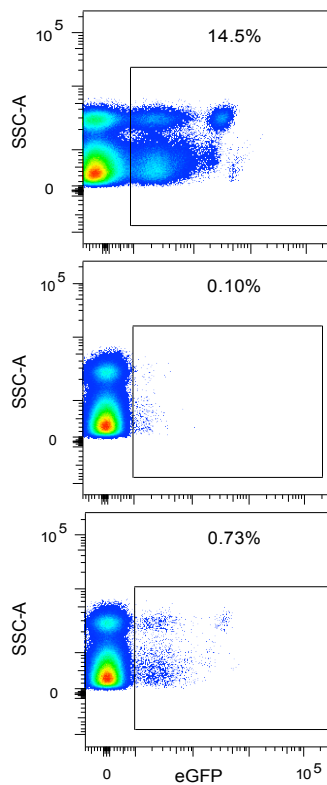


16 wks Post BMT Engrafted

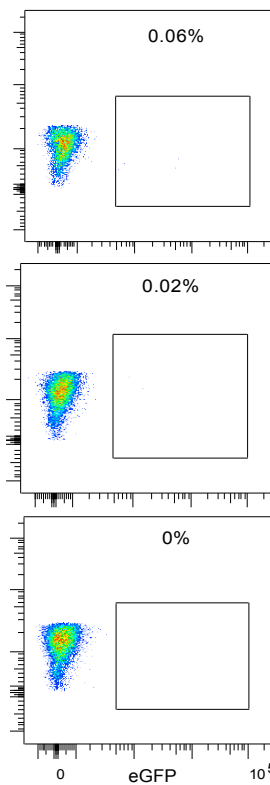
D. Recipient WBM



E. PBMC



F. Lung



**Supplemental Figure 10. Related to Figures 1, 4&5. Bone Marrow Transplantation analyses reveal that tissue resident adult lung MPC are NOT derived from *Abcg2* expressing HSC in bone marrow.** Mice were induced with intraperitoneal tamoxifen (0.5mg total). **A&B.** 2 weeks or 7 weeks post-lineage labeling whole bone marrow (WBM) and peripheral blood mononuclear cells (PBMC) were analyzed by flow cytometry to detect and enumerate eGFP positive cells. **C.** PBMC from uninduced reporter mice (used as recipients) were analyzed as a baseline negative control. **D-F.** WBM was harvested from 5 induced mice and  $\times 10^6$  cells/mouse transplanted into 3 lethally irradiated recipient  $^{flstopfl}$  mTomato/meGFP mice that received 11Gy in a split dose. **D&E.** 16 weeks post transplant WBM and PBMC were analyzed to confirm and quantify engraftment of ABCG2 eGFP labeled WBM and HSC derived circulating blood lineages. **F.** Lung tissue was isolated from the recipient mice, digested to obtain a single cell suspension, and one million total cells were analyzed by flow cytometry to detect CD45<sup>neg</sup> eGFP<sup>pos</sup> labeled cells.

**Supplemental Table 1. Lineage Analysis of Adult Mesenchymal Populations**

Lineage Trace Marker	Human Equivalent Identified	Protein	Putative Cell Population Tracing	Specificity of Marker	Reported Homeostatic Function (Adult Lung)	Refs.
<b>ABCG2</b>	<b>YES</b>	MDR transporter	*Lung MPC/pericyte progenitors	*Adult mesenchymal pericyte progenitors <b>* activated pericytes</b>	Regulate <b>microvascular</b> integrity and function	(1-6)
<b>Gli1</b>	NO	Transcription factor, associated with sonic hedgehog signaling	Lung MSC, lung mesenchyme, fibroblasts	Mesenchyme, fibroblasts/pericytes <b>*myofibroblasts, epithelial progenitors, lung cancers</b>	ND	(7-12)
<b>Tbx4</b>	NO	T-box family Transcription factor	Developing lung mesenchyme (vascular precursors), <b>*adult lung mesenchyme</b>	Smooth muscle, endothelium, fibroblasts, pericytes, vascular progenitors <b>* myofibroblasts</b>	ND	(13-16)
<b>Foxd1</b>	NO	Forkhead family Transcription factor	Foxd1 pericytes	Developing vascular/ mesenchymal lineages, pericytes, endothelium <b>*myofibroblasts</b>	ND	(17, 18)
<b>PDGFRb</b>	<b>YES</b>	Tyrosine kinase receptor for PDGFB	SMC precursors	Fibroblasts, mesenchyme, differentiated pericytes, progenitors <b>*myofibroblasts * activated pericytes</b>	Diverse mixed population	(19-21)
<b>NG2 (cspg4)</b>	NO	Neural/glia antigen 2, membrane proteoglycan	Differentiated pericytes	Differentiated pericytes Neural precursors <b>* activated pericytes</b>	ND	(22, 23)
<b>Tbx18</b>	NO	T-box family Transcription factor	Differentiated pericytes	Differentiated pericytes, smooth muscle, glomerular mesangial cells	NO	(24, 25)
<b>SMA (acta2)</b>	NO	Conserved protein involved in cytoskeletal structure and integrity	Vascular SMC	Differentiated pericytes, smooth muscle, <b>*myofibroblasts</b>	ND	(26, 27)
<b>ADRP</b>	NO	Perilipin2, adipose differentiation related protein	Lipofibroblasts/myofibroblasts	Alveolar typeII cells Lipofibroblasts <b>*myofibroblasts</b>	Fat storage for surfactant synthesis	(27, 28)

**\* in response to injury**

\* based on low dose TAM as published

**Supplemental Table 2. Cell Surface Determinant Expression by Primary Human Lung Mesenchymal Progenitors**

<b>%</b>	<b>CD44</b>	<b>CD73</b>	<b>CD105</b>	<b>CD106</b>	<b>CD146</b>	<b>CD140b</b>	<b>CD 140a</b>	<b>CD45</b>	<b>CD14</b>	<b>CD31</b>	<b>CD34</b>
<b>Control</b>	99.0	99.4	98.6	6.50	53.2			0	0	0.02	0
<b>Control</b>	99.9	99.8	99.2	9.91	73.4	90.4	0.41	2.96	0.06	0.11	0.06
<b>Control</b>	99.8	100	99.9	0.44	33.1	99.9	0.37	0.01	0	0.02	0.07
<b>Control</b>	98.9	99.9	99.9	0.46	31.3	99.5	0.22	0	0.01	0	0.04
<b>Control</b>	100	100	100	3.73	5.31	95	1.28	0.03	0	0	0
<b>HPAH</b>	100	100	100	7.64	63.1	90.2	10.7	0	0	0	0
<b>HPAH</b>	100	100	98.6	5.83	1.67	73.1	0.01	0.1	0	0.04	0
<b>IPAH</b>	99.9	99.6	96.9	9.74	72.3	93.2	12.1	0.08	0.02	0	0.02
<b>IPAH</b>	99.1	99.7	83.6	0.72	53.8	97	0.19	0.03	0	0.03	0.02
<b>IPAH</b>	100	100	100	30.2	36.8	98.8	0.05	0.18	0.03	0.01	0.01
<b>PVOD</b>	100	100	100	0.021	58.9	97	0	0.03	0	0	0.02
<b>IPF</b>	100	100	99.6	0.66	23.3	98.6	0.84	1.39	0	0.54	0.07
<b>IPF</b>	100	99.9	99.9	2.73	28	91.9	1.3	1.96	0	0.36	0.19
<b>IPF</b>	100	100	79.3	20.7	56	95.2	0.97	0.25	0.04	0.11	0.18
<b>IPF</b>	100	100	100	5.8	68	97.3	1.62	0.41	0.19	0.25	0.21
<b>IPF</b>	100	99.9	99.8	3.17	30.1	93.6	9.3	0	0.50	0.03	0.36
<b>IPF</b>	100	100	99.9	18.2	37.1	94.6	4.7	2.48	0.27	0.50	0.50
<b>IPF</b>	100	99.9	99.8	1.95	1.36	97.5	21.1	0.12	0.01	0	0.15
<b>IPF</b>	100	99.9	99.9	0.23	2.69	97.6	14.2	0.01	0.01	0	0.12
<b>IPF</b>	100	99.7	100	0.42	23.2	99.3	4.07	0.41	0	0.01	0.01

**Supplemental Table 3. Changes in Gene Expression by human IPF MPC relative to Control**

<i>GENE SYMBOL</i>	<b>Fold Change</b>	<b>P.Value</b>			
<i>A2M</i>	-10.70467529	0.036500923032124	<i>SNORD116-1</i>	-2.140822916	0.0495231874593133
<i>FGL2</i>	-7.693967704	0.0256072906383432	<i>CXCL8</i>	-2.137192588	0.0100322358920139
<i>CCDC68</i>	-5.473230716	0.016807460293437	<i>SNORD116-5</i>	-2.135660937	0.0292456352355185
<i>CCND2</i>	-5.209821687	0.0380580582751768	<i>RNU6-532P</i>	-2.129942864	0.0494828121454666
<i>TBX4</i>	-5.019948274	0.0448110586413518	<i>DNER</i>	-2.100643977	0.00661795200839857
<i>RGS2</i>	-4.619624478	0.0445186547054985	<i>RNU6-994P</i>	-2.096124898	0.000752295712560894
<i>AREG</i>	-4.290845526	0.0229133095301039	<i>RNU6-256P</i>	-2.081742188	0.0192187654569144
<i>HGF</i>	-4.253575244	0.0420918038386606	<i>BNC1</i>	-2.06286964	0.00349167388031037
<i>ADAMTS19</i>	-3.969265146	0.00201148272730408	<i>ANO4</i>	-2.026480497	0.000574139893916889
<i>PLAT</i>	-3.892361379	0.0021086826277054	<i>FLRT2</i>	-2.025851078	0.0012794458899611
<i>MAOA</i>	-3.777264264	0.0084799822051779	<i>OXR1</i>	-2.013414105	0.000706733766683373
<i>ZNF804A</i>	-3.678875524	0.00809196340407516	<i>ANXA3</i>	-2.010083919	0.0345842314444903
<i>AREG</i>	-3.66547419	0.029944850543154	<i>TMTC1</i>	-2.007540041	0.0470908212957579
<i>EIF4A2</i>	-3.651110628	0.044012521569329	<i>SERPINI1</i>	-1.986606922	0.0191944345904753
<i>SHC4</i>	-3.630887907	0.0282372947165337	<i>SNORD116-29</i>	-1.980518512	0.0403258310606488
<i>CLDN1</i>	-3.4970137	0.037144542156085	<i>OGFRL1</i>	-1.973048363	0.035141568518173
<i>LIF</i>	-3.480421714	0.0316795316818668	<i>MANSC1</i>	-1.955688586	0.00100344844622094
<i>SCG2</i>	-3.142817629	0.0290668333656887	<i>RNF152</i>	-1.951366407	0.00446031906327883
<i>NPHP3-ACAD11</i>	-2.84601388	0.00930155643330746	<i>RNU6-943P</i>	-1.94697858	0.0104715804180039
<i>P4HA3</i>	-2.827311821	0.0217121968333358	<i>CREB5</i>	-1.928200636	0.014372117490436
<i>MFSO6</i>	-2.788701833	0.0221254210189471	<i>SORT1</i>	-1.925176462	0.00279618887154823
<i>HSD17B2</i>	-2.7732347	0.0473629350079755	<i>SVIL</i>	-1.921737949	0.00631110342162366
<i>RASSF2</i>	-2.746479006	0.000948624059334548	<i>ATL1</i>	-1.919385185	0.0406458270342084
<i>ETV1</i>	-2.727339376	0.0477134073330072	<i>CSGALNACT2</i>	-1.903472092	0.0357402689512998
<i>DOCK4</i>	-2.694984372	0.0174729677218037	<i>SNORD116-4</i>	-1.890806876	0.0113742537748088
<i>MT-TT</i>	-2.667884445	0.00543143167356641	<i>CHAC1</i>	-1.890717874	0.00437602036875792
<i>LRCH2</i>	-2.619952731	0.0286483134540876	<i>ZBTB8OSP2</i>	-1.867947335	0.0305574351259457
<i>SYT1</i>	-2.618758702	0.0326665674110781	<i>HLA-DMA</i>	-1.867173834	0.011952605
<i>ABCC4</i>	-2.579808561	0.000920040489812247	<i>HLA-DMA</i>	-1.867173834	0.011952605
<i>SGIP1</i>	-2.557664779	0.0349063809958603	<i>GNAI1</i>	-1.867149708	0.00198598183568132
<i>KCNJ2</i>	-2.533791795	0.0423920315238724	<i>SNORD116-21</i>	-1.855282478	0.0218411763016107
<i>PGM2L1</i>	-2.490522631	0.0152380424107094	<i>UBA5</i>	-1.855245283	0.00720856846875252
<i>BTG1</i>	-2.483931987	0.041003248	<i>MGST2</i>	-1.853976628	0.00303822449154642
<i>RDH10</i>	-2.47580547	0.00942435274733527	<i>HLA-DMA</i>	-1.827652916	0.013042199150698
<i>FHL1</i>	-2.430044199	0.000699336089577674	<i>ANKRD29</i>	-1.814913456	0.0351636587146933
<i>PLK2</i>	-2.425807371	0.000167554342986324	<i>ANKRD36C</i>	-1.809417847	0.0264693515830586
<i>CHL1</i>	-2.350607534	0.024969777398051	<i>RNY4P23</i>	-1.804465914	0.00298891635710363
<i>VWA5A</i>	-2.314166288	0.020327773535249	<i>PHLDA1</i>	-1.803774881	0.0406671781250576
<i>SEZ6L2</i>	-2.308166722	0.0040036123292153	<i>TNFRSF19</i>	-1.79025651	0.0429940782881568
<i>GLB1L</i>	-2.293463091	0.0161785094690692	<i>PAM</i>	-1.763915514	0.00588153799161291
<i>VPS29</i>	-2.263101651	0.0089677963836694	<i>RN7SL5P</i>	-1.76044875	0.0047469167041867
<i>AGPAT9</i>	-2.257336013	0.00808685661122118	<i>SNORD116-14</i>	-1.749424087	0.0243777313677153
<i>ACSS3</i>	-2.244778035	0.00157852312223834	<i>PDK4</i>	-1.743210925	0.00582319863149421
<i>SFRP1</i>	-2.217445343	0.0132155455448372	<i>LRRIC7</i>	-3.633323833	0.0404700301012512
<i>LRRK2</i>	-2.211497304	0.0111664324790173	<i>SERPING1</i>	-2.658407666	0.0458323957181124
<i>LIMD1-AS1</i>	-2.172551351	0.032274485931241	<i>TNXB</i>	-2.198901204	0.0382066277571796
<i>GPX3</i>	-2.171993568	0.0333608137990811	<i>EFCAB4B</i>	-2.040657876	0.0233718172222625
<i>ROBO2</i>	-2.160982253	0.00874779527221622	<i>DKK1</i>	-2.020254141	0.0411683778146618
<i>GPR37</i>	-2.153880564	0.028571921450456	<i>SNX29P2</i>	-1.963058853	0.00252020756443324
<i>PCDHB5</i>	-2.146923019	0.0428873529280663	<i>SLIT3</i>	-1.901070997	0.0176942057174128
<i>SNORD64</i>	-2.144841182	0.0253442957778582	<i>EFEMP1</i>	-1.890407382	0.0463666170125491
<i>PLEKHH2</i>	-2.144416246	0.033506649178532			

<b>GENE SYMBOL</b>	<b>Fold Change</b>	<b>P.Value</b>
GRAMD3	1.747452668	0.0045518603328891
ARHGAP11A	1.750150267	0.0140936718559253
GCNT4	1.751914978	0.0466649125772611
PAPSS2	1.753250664	0.0366947322886239
ANKRD30B	1.758576631	0.0470800319234054
WNK4	1.760949916	0.00235448564907887
TLR4	1.761048652	0.00177315299460159
PII6	1.767725974	0.0297986517125782
AFAP1	1.770633321	0.0222227734810526
BLVRB	1.772099055	0.00758142537663843
DSEL	1.779090451	0.0345517597073478
HMGCS1	1.791772362	0.0107684319906305
ARHGAP23	1.791973584	0.00258926501759127
DIO2	1.797479125	0.016099976207137
GALNT15	1.800252765	0.00479134135014547
MARCH3	1.807503989	0.0197711364412445
CORIN	1.863703209	0.0386603991616007
KIAA1549L	1.866646595	0.00589383627851261
LRIG3	1.878948043	0.0060785756682511
GXYLT2	1.879270556	0.0305741235800834
RN7SL441P	1.903944052	0.00203576338795186
KRT18P49	1.913819646	0.00235806536546106
PPAPDC1A	1.934475792	0.0216809938823747
RAC2	1.937050001	0.0155090071871399
ADAMTS2	1.95067279	0.00534818945708477
SEMA7A	1.955830866	0.0285934672758101
ANKH	1.975366441	0.0100881841630165
LCE2D	1.980820673	0.00114242614000432
PLA2G5	2.010414903	0.0382643488296092
LOC728323	2.021475546	0.00700410832643984
LRRC17	2.023581832	0.00435678659114876
ALDH1L2	2.040131168	0.0396986731031911
PPP4R4	2.09277526	0.000759740277445238
PMP22	2.115931457	0.00718894877123754
KCND2	2.118581431	0.0418865757232186
TRPV2	2.123199685	0.0196601880680548
RNA5SP55	2.147598699	0.000376881960677568
MGARP	2.167534851	0.00909228748949302
FRMD6	2.173124345	0.0435731916592436
PODXL	2.205591561	0.00042135313173675
IFIT3	2.208374104	0.0313487891876363
STEAP2	2.209570732	0.0212213115846192
PSG7	2.255351371	0.0219699747746957
MYPN	2.257212655	0.0191748455122558
SNAI2	2.31265887	0.0432647956435016
OSR1	2.317216821	0.00827163895500385
BAMBI	2.334667108	0.00582034723138349
MYO1D	2.360712465	0.0111363695261108
IFIT2	2.373810217	0.0476660033675746
IFIT1	2.406578596	0.0137142318834885
COL3A1	2.420111278	0.000677615093287991
KCNK2	2.428593149	0.0253470319166521
NEO1	2.451865284	0.00978258465303627

STEAP1	2.473460604	0.00715158455125515
DOCK10	2.510802883	0.0221494895854914
ALPK2	2.528951789	0.0095137854727379
COL1A1	2.57006106	0.000659385147694621
PSG1	2.654460061	0.0438449606557497
DSP	2.691125569	0.00772523380452655
RTN1	2.89802229	0.0343036096036955
LUM	2.921075358	0.0409201007778163
STARD5	2.943083377	0.0485005076372402
DSG2	3.015286849	0.00113343948869569
PRPS1	3.384573986	0.0374366153256767
ITGAI1	3.646860111	0.0279677862582794
NRXN3	3.814486064	0.00339722115739204
CYP11B1	4.366813105	0.000331024716799638
BGN	4.765800214	0.00364236771997039
CD36	4.871067482	0.0169232776758505
PSG4	5.342145846	0.0366308293723663
ABI3BP	5.748366917	0.0332404389719987
HAS2	6.209922307	0.000416432239906776
SULF1	6.472891815	0.0470363264100581
GPNUMB	7.490695677	0.020197492658232
NEFM	9.269205603	0.0441305859157239
MFAP5	17.73043038	0.00638433409483308
POSTN	20.41113402	0.00479973524453205
PCYT1A	1.747591268	0.0403990900330329
BTBD3	1.784702521	0.0349762203267408
LMO7	1.796798062	0.021829691711803
TNSI	1.826419144	0.0135815722784535
PARP3	1.839744738	0.0352145968245071
NAAA	1.863045509	0.00794892513324626
FSTL3	1.868069842	0.0239134367246111
FCSD2	1.902686782	0.00381588584475335
PLA2G15	1.907563238	0.0412152160808909
NEO1	1.943790204	0.00371190481184341
CCND3	1.952421484	0.0271533008140867
TRIM22	1.972691124	0.0475591084480264
TAGLN	2.00380984	0.00230134804094855
TPM2	2.007370017	0.0253447738367225
NOX4	2.026852713	0.00542348699861012
B3GAT3	2.101991789	0.029346641402275
EDNRA	2.10692064	0.0204506419772496
DUSP1	2.122564324	0.00849440854400922
SERINC2	2.131829275	0.0441561221247797
ERRFI1	2.173655641	0.0220897002616097
SORT1	2.234163252	0.000441242013950866
PDCD1LG2	2.241985905	0.044581165767895
SHC4	2.252737378	0.0119506201412501
GCNT4	2.32944618	0.0146313468950811
CDC42EP3	2.356661887	0.0322911442054045
GABARAPL1	2.366662554	0.0398248508214021
EFNB2	2.386022819	0.0468756602715561
MIR221	2.446368543	0.0334604560546797
TM6SF1	2.566845221	0.00878191943831793
WNT5A	2.570760319	0.0355291624181085

<i>GAS6</i>	2.629289473	0.029471799041216
<i>STC1</i>	2.642403869	0.0309366964626144
<i>MGAT5</i>	2.720034448	0.00918867133676521
<i>LMOD1</i>	2.771107661	0.00144450378688513
<i>TRPV2</i>	2.798650968	0.0315225683754965
<i>RNA5SP155</i>	2.842075999	0.0284914797903674
<i>HAPLN3</i>	2.850473261	0.0194412609127543
<i>ANGPT1</i>	2.882469992	0.0204597516636323
<i>BDNF</i>	2.994426179	0.0253918899358664
<i>CCDC68</i>	3.051610691	0.0165556560685105

<i>ARHGDIB</i>	3.823603981	0.0493381377140052
<i>CHAC1</i>	3.959435672	0.0119703030657053
<i>ACTG2</i>	3.990322751	0.0191152962551271
<i>ACTA2</i>	4.197448808	0.0128918440377968
<i>EDN1</i>	4.526301198	0.00151911038268212
<i>MMP3</i>	4.535691791	0.00524789676140419
<i>CORIN</i>	4.729458443	0.0468724685463078
<i>WFDC1</i>	5.342014286	0.0270701903362325
<i>MAMDC2</i>	6.519398079	0.00118105729551713
<i>ALDH1A1</i>	9.969861395	0.014766744875251

**Supplemental Table 4. Antibody Specifications**

Smooth Muscle Actin	M0851	DAKO, Carpinteria, CA
Wisp1	18166-1-AP	VWR, Radnor, PA
Cyclin D1	2978	Cell Signaling Technology, Danvers, MA
B-catenin (total)	8480	Cell Signaling Technology, Danvers, MA
B-catenin (active)	8814	Cell Signaling Technology, Danvers, MA
PCNA	M3619	DAKO, Carpinteria, CA
BMPR2	PIMA515826	Fisher, Hampton, NH
B-actin	Ab8227	Abcam, Cambridge, United Kingdom
Donkey anti-Rabbit HRP	711-035-152	Jackson ImmunoResearch, West Grove, PA
GFP	NB600-308	Novus, Saint Charles, MO
NG2	PA5-17199	Thermo Fisher, Waltham, MA
Factor 8	A0082	DAKO, Carpinteria, CA

*Murine flow cytometry*

CD45-APC	17-0451-83	eBioscience, San Diego, CA
TER119	48-5921-82	eBioscience, San Diego, CA
CD105-APC	120413	Biolegend, San Diego, CA
CD73-APC	127209	Biolegend, San Diego, CA
CD146-APC	134711	Biolegend, San Diego, CA
CD140a-APC	135907	Biolegend, San Diego, CA
CD140b-APC	136007	Biolegend, San Diego, CA
CD44-APC	103011	Biolegend, San Diego, CA
CD F4/80-APC	17-4801-80	eBioscience, San Diego, CA
CD45-APC –eF780	47-0451-82	eBioscience, San Diego, CA
CD14-APC	17-0141	eBioscience, San Diego, CA
Sca-1-PE	12-5981-82	eBioscience, San Diego, CA
c-kit-APC	17-1171-81	eBioscience, San Diego, CA
CD106	105717	Biolegend, San Diego, CA
CD3-APC	17-0032	eBioscience, San Diego, CA

*Human flow cytometry*

CD45-APC	17-9459-42	eBioscience, San Diego, CA
ABCG2-PE	12-8888-82	eBioscience, San Diego, CA
CD144-PE	12-1449	eBioscience, San Diego, CA
CD105-PE	12-1057	eBioscience, San Diego, CA
CD106-PE	12-1069	eBioscience, San Diego, CA
CD140A-PE	556002	BD Pharmingen, San Jose, CA
CD140B-PE	558821	BD Pharmingen, San Jose, CA
CD31-FITC	11-0319	eBioscience, San Diego, CA
CD146-FITC	11-1469	eBioscience, San Diego, CA
CD34-FITC	11-0349	eBioscience, San Diego, CA
CD14-FITC	11-0149	eBioscience, San Diego, CA
CD44-FITC	11-0441	eBioscience, San Diego, CA
CD73-APC	17-0739	eBioscience, San Diego, CA

*Secondary Abs*

anti-rat igG	A-110007	Invitrogen, Waltham, MA
anti-rabbit igG	A-11012	Invitrogen, Waltham, MA
anti-mouse igG	A-11005	Invitrogen, Waltham, MA
anti-rat igG	A-11006	Invitrogen, Waltham, MA
anti-mouse igG	A-11029	Invitrogen, Waltham, MA
anti-rabbit igG	A-11008	Invitrogen, Waltham, MA
anti-goat igG	A-11078	Invitrogen, Waltham, MA

**Supplemental Table 5. qPCR Primers Specifications**

<b>Murine</b>	forward	reverse
<i>HPRT</i>	AGTCCCAGCGTCGTGATTAG	TCTCGAGCAAGTCTTTCAGTCC
<i>BMPR2</i>	GTGTGCTGAGGAGAGGATGG	ACATTGGGTTGACCGTTGGG
<i>cspg4 (NG2)</i>	TCAACAGCGCCAGCTATCTC	CGGCCATGAAGTAGGTCCTC
<i>acta2 (SMA)</i>	GGCTTCGCTGTCTACCTTCC	AGTTGTGTGCTAGAGGCAGAG
<i>wisp1</i>	CCGTGGAGCAACGGTATGAG	ACCGGGCATTGACGTTAGAG
<i>ccnd1 (Cyclin D1)</i>	GCGTACCCTGACACCAATCTC	CTCCTCTTCGCACTTCTGCTC
<i>fibronectin</i>	TTCAAGTGTGATCCCCATGAAG	CAGGTCTACGGCAGTTGTCA
<i>coll1a1</i>	GCTCCTCTTAGGGGCCACT	CCACGTCTCACCATTGGGG
<i>col3a1</i>	CAAGGCTGCAAGATGGATGC	TGTCCACCAGTGCTTACGTG
<i>sFRP1</i>	Mm00489161_m1	Applied Biosystems, Foster City CA
<i>sFRP2</i>	GCGACCTCATTTCCGGTTTC	CAGCTATGGGTTTCCAAGGC
<i>rgs5</i>	GAACCTGGTGGAAACCGTCTC	TGGAAGCCTGACCAGATGAC
<i>ctnbl1 (b-catenin)</i>	AGCTCGTGTCTGTGAAGCC	GGATGAGCAGCGTCAAACCTG
<i>axin2</i>	TGAGATCCACGGAACAGC	GCTGGTGCAAAGACATAGCC
<i>dkk1</i>	Mm00438422_m1	Applied Biosystems, Foster City CA
<i>GAPDH</i>	4352339E	Applied Biosystems, Foster City CA
<b>Human</b>		
<i>HPRT</i>	CCCTGGCGTCGTGATTAGTG	TCGAGCAAGACGTTTCAGTCC
<i>NG2</i>	CTTTGACCCTGACTATGTTGGC	TGCAGGCGTCCAGAGTAGA
<i>SMA</i>	CCTTTGGCTTGGCTTGTGTCAG	GGTGCGGACAGGAATTGAAG
<i>Wisp1</i>	AGGAACTGCATAGCCTACACA	TGGTACACAGCCAGACACTTC
<i>Cyclin D1</i>	GCTGCGAAGTGGAACCATC	CCTCCTTCTGCACACATTTGAA
<i>TNC</i>	TGCGAAGAAGGCTTCACA	TACACATTTGCCCTCGACAC
<i>SPON2</i>	CGGCCAAATACAGCATCACC	CCCAGCAGCGAAGACCACT
<i>NEO1</i>	GGAGCCGGTGGATACACTCT	TGGCGTCGATCATCTGATACTA
<i>RGS5</i>	Hs10591223_s1	Applied Biosystems, Foster City CA
<i>PTGS2</i>	Hs00153133_m1	Applied Biosystems, Foster City CA
<i>PEAR1</i>	Hs01378394_m1	Applied Biosystems, Foster City CA
<i>Dkk1</i>	Hs00183740_m1	Applied Biosystems, Foster City CA
<i>GAPDH</i>	4326317E	Applied Biosystems, Foster City CA

## Supplemental Experimental Procedures

**Genetic manipulation of murine ABCG2<sup>pos</sup> mesenchymal progenitors.** All procedures and protocols were approved by the Institutional Animal Care and Use Committee at Vanderbilt University. ABCG2-Cre<sup>ERT2</sup> mice, a generous gift of Dr. B. Sorrentino (29), were crossed to a fluorescent eGFP reporter (Cg)-Gt(ROSA)26Sortm4(ACTB-tdTomato,-EGFP) JAX stock# 007676; designated mT/mG strain to facilitate lineage analysis and quantitation via eGFP expression. A third gene was crossed into the mice to knockout Bmpr2 (<sup>fl<sup>oxp</sup></sup>Bmpr2 (30)), or overexpress bcatenin/Wnt (Catnb<sup>lox<sup>p</sup></sup>(Dex3) (31). Mice were injected intraperitoneally at 8-10 weeks of age with a low dose (0.5mg) tamoxifen (T-5648; SIGMA, St. Louis MO) in sesame oil, or sesame oil alone (vehicle control) as described (1, 3). The mice were randomized and distributed as 3-5 mice per cage for studies.

**Phenotyping of pulmonary vascular dysfunction.** Vascular permeability in the lungs was quantitated using an AngioSense 750EX Fluorescent Imaging Agent (Perkin Elmer, Waltham) with spectroscopic imaging in a Pearl Impulse Small Animal Imager (LI-COR, Lincoln) as previously described (32). Images were analyzed using Image Studio software (LI-COR, Lincoln) and total fluorescence of lung area was normalized to total fluorescence of the nose. The number of subjects per group were 5-10. Elevated pulmonary artery pressure was documented indirectly by the measurement of right ventricular systolic pressure (RVSP) as previously described (33). Five independent experiments were pooled for the hemodynamic measurements. Baseline pressures were measured and epinephrine [30mg/18g mouse] was injected intravenously into the femoral vessel. RVSP was measured at the time of harvest or 20 weeks (following tamoxifen induction) (2, 33). The number of subjects per group was 5-10. Histologic endpoints included muscularization and microvessel density of the distal microvessels by immunostaining to detect smooth muscle actin (SMA) or Factor 8 on 5-8 mice per group (33). Morphometric assessment consisted of the determination of the average interalveolar distance by mean linear intercept (MLI) (34) using H&E-stained lung sections from 6-8 wild type or transgenic mice. For each pair of lungs, 40 histological fields were photographed and evaluated in a blinded fashion. Immunofluorescent staining was performed to lineage trace eGFP-labeled lung mesenchymal progenitors and localize smooth muscle alpha (SMA), reagents outlined in **Supplemental Table 1**.

**Isolation and Characterization of Primary Lung mesenchymal progenitors.** Human lung plastic adherent cells were isolated from explant lung tissue post autopsy or transplant by collagenase digest (Vanderbilt IRB Protocol 9401) to form a suspension. The cells were stained with antibodies to sort CD45<sup>neg</sup> ABCG2<sup>pos</sup> cells (lung mesenchymal progenitors) using a BD FACSAria III (BD Biosciences, San Jose, California). Fluorescent minus one (FMO) and IgG2b isotype (eBioscience, San Diego, California 12-8888-82) controls were used to set the ABCG2-PE gates. DAPI was used to exclude dead cells. The compensation controls were established as cells only, cells + DAPI, cells + APC-CD45 antibody, and cells + PE-ABCG2 antibody, alternatively comp beads were used. The gating strategy routinely included FSC/SSC, Single cells gated by SSC-Width (SSC-W)/SSC-Height (SSC-H), FSC-W/FSC-H, DAPI+Ter119 to gate out dead and red blood cells followed by gating on the CD45 negative population. The sort sample consisted of cells + DAPI + APC-CD45 antibody+ PE-ABCG2 antibody. A summary of human lung mesenchymal progenitors lines is presented in **Table 1**.

All animal procedures adhered to the Vanderbilt University IACUC guidelines. Murine lung mesenchymal progenitors were isolated from induced ABCG2 Cre<sup>ERT2</sup> x mT/mG mice using a BD FACSAria III (BD Biosciences, San Jose, California) to identify eGFP positive cells. Isolated cells were plated on attachment factor-coated dishes, expanded and analyzed at passage 7. Gating strategies included FSC/SSC, dead cell exclusion with DAPI, red blood cell exclusion with Ter119 and doublet discrimination. Gates were set using FMO controls including cells isolated from uninduced mice expressing mTomato. Each sample was mixed well and incubated for 20 minutes at room temperature with conjugated antibodies. DAPI was used to exclude dead cells. Following expansion all primary human and murine mesenchymal progenitors were analyzed by flow cytometry to confirm the presence of CD105, CD106, CD73, Sca1, CD44 and the absence of c-kit, CD14 and CD45 (**Supplemental Table 1**) using a BD Fortessa or LSRII (BD Biosciences, San Jose, California).

To compare relative growth characteristics of mesenchymal progenitors and colony forming unit - fibroblast colonies (CFU-F), cells were counted using the Countess (Life Technologies, Grand Island, NY) and diluted to a concentration of 6x10<sup>3</sup>/ml. 1 ml of the cell suspension was added to individual gelatin-coated plates containing 10 ml  $\alpha$ -MEM with 20% fetal bovine serum. The plates were gently rocked to distribute the cells evenly. Cells were cultured for 5-10 days (depending on colony size), changing media every 48 hours. After colonies were formed, spent medium was removed and cells washed once with DPBS. 4% paraformaldehyde was used to fix the cells for 20 minutes. Following a PBS wash, Giemsa stain (Sigma Aldrich, Saint Louis, MO; Cat# GS500) was added to cover cells overnight. Giemsa stain was then removed and the plates gently washed with water. Plates were allowed to air dry, and colonies of 50 cells or larger were enumerated. Cell enumeration assays were performed by seeding mesenchymal progenitors at 50,000 cells per well in duplicate for collection time points at 24, 48 and 72 hours. At each time point, the spent medium was removed, and cells washed with DPBS. Cells were collected, washed with PBS and re-suspended in 0.5 ml  $\alpha$ -MEM. 10 $\mu$ l of the cell suspension was counted using the Countess (Life Technologies, Grand Island, NY) per manufacturers instructions. The assay was performed in triplicate thrice independently.

**In vitro Contraction.** To test the contractility of ABCG2<sup>pos</sup> mesenchymal progenitors in response to treatments cells were plated on collagen discs and photographed over time. Briefly, 80% 3mg/ml bovine collagen solution (Advanced Biomatrix, San Diego, CA; Cat# 5005-B), 10 % 10x DPBS (Life Technologies, Grand Island, NY; Cat# 14200-166), and 10% 0.1 M NaOH (Thermo Fisher Scientific, Fair Lawn, NJ; Cat# BP359-500) was carefully added to the center of Teflon rings (Seastrom Manufacturing, Twin Falls,

Idaho; Cat# 5612-303-62) in suspension 6 well plates (Sarstedt, Germany; 83.3920.500). The gels were allowed to set at 37°C and 5% CO<sub>2</sub> for 1 hour. ABCG2<sup>pos</sup> mesenchymal progenitors were plated at 10,000 cells per collagen gel. The gels were then incubated at 37°C and 5% CO<sub>2</sub> for 30 minutes to allow cells to adhere. Each treatment condition was then established and the gels were incubated for another 30 minutes. After 30 minutes, the gels were photographed at the 0 hour time point. The gels were then photographed at the 24, and 48-hour time points. Image J was used to calculate the area in pixels squared of each gel at each time point. The fold change in pixel squared for the 24 and 48 time points was calculated as a ratio to the gel area at the 0 hour time point.

**Modulation and Detection of BMPR2 and Wnt Signaling.** To determine the cellular response to the BMPR inhibitors dorsomorphin (DM) or 4-[6-[4-(1-Methylethoxy)phenyl]pyrazolo[1,5-*a*]pyrimidin-3-yl]-quinoline (DMH1), mesenchymal progenitors were plated at a concentration of 60,000 cells per well in medium containing 20% serum. The cells were allowed to remain in 20% serum medium for 24 hours. After 24 hours, the medium was changed to 20% serum treatment medium containing DM (5mM), DMH1 (10mM), or DMSO vehicle (4). RNA lysates were collected at 48 hours and protein lysates were collected at 72 hours for analyses of gene and protein expression.

Dual luciferase analysis was utilized to detect changes in BMPR2 and Wnt signaling activity. ABCG2<sup>pos</sup> mesenchymal progenitors were plated onto 12-well plates at 3x10<sup>4</sup> cells per well. After 24 hours, ABCG2<sup>pos</sup> mesenchymal progenitors were co-transfected with TOPflash and *Renilla* transfection control plasmids or BRE reporter plasmid [1.6 mg/well] with *Renilla* reporter plasmid co-transfected at 1:20, according to lipofectamine 2000 protocol (Life Technologies). Cells were incubated with lipofectamine 2000 for 5 hours before transfection media was replaced with cell media (4). After 24 or 48 hours, lysis buffer was added to cells, and then firefly and *Renilla* luciferase activity was measured according to Dual-Luciferase Reporter Assay System protocol (Promega) using a GloMax-Multi Detection System (Promega). TOPflash experiments were normalized to co-transfected *Renilla* gene expression. Luciferase experiments were repeated thrice independently.

**Western Blot Analysis.** Protein extracts were made by scraping cells in RIPA buffer (Cell Signaling, Boston, MA; cat # 9806S) containing protease and phosphatase inhibitors (ThermoFisher Scientific, Waltham, MA; cat # 78444). After determination of protein concentrations and standardization, cell lysates were mixed with an equal volume of Laemmli SDS loading buffer, resolved on 10% polyacrylamide-SDS gels and transferred to PVD membranes. The blots were blocked with phosphate buffered saline (PBS) containing 5% dry milk and 0.1% Tween 20, and then treated with antibodies that detect the target proteins as labeled in the figures overnight at 4°C. The blots were washed and subsequently treated with appropriate secondary antibodies conjugated to horseradish peroxidase. After the blots are washed, specific immune complexes were visualized with SuperSignal West Pico Chemiluminescent Substrate (**Supplemental Table 1**).

**Imaging.** Epifluorescent and brightfield images were captured with Nikon Eclipse 90i upright epifluorescence or Nikon Eclipse TS100 microscopes. Confocal imaging was performed using a Nikon Eclipse Ti. Fluorochromes used included DAPI (to label nuclei), secondary antibodies conjugated to Alexa 488 or Alexa 594 (ThermoFisher, Hampton, NH) to detect SMA, factor VIII, GFP, cnd1/cyclinD1 or active b-catenin (**Supplemental Table 1**). The camera used to capture the images was a Nikon DS-Fi1 using the Nikon NIS elements AR 4.11.00 acquisition software.

## Supplemental References

1. Chow K, Fessel JP, KaoriIhida S, Schmidt EP, Gaskill C, Alvarez D, Graham B, Harrison DG, Wagner DH, Nozik-Grayck E, et al. Dysfunctional resident lung mesenchymal stem cells contribute to pulmonary microvascular remodeling. *Pulmonary Circulation*. 2013;3(1):31-49.
2. Jun D, Garat C, West J, Thorn N, Chow K, Cleaver T, Sullivan T, Torchia EC, Childs C, Shade T, et al. The Pathology of Bleomycin-Induced Fibrosis Is Associated with Loss of Resident Lung Mesenchymal Stem Cells That Regulate Effector T-cell Proliferation. *STEM CELLS*. 2011;29(4):725-35.
3. Marriott S, Baskir RS, Gaskill C, Menon S, Carrier EJ, Williams J, Talati M, Helm K, Alford CE, Kropiski JA, et al. ABCG2(pos) lung mesenchymal stem cells are a novel pericyte subpopulation that contributes to fibrotic remodeling. *American Journal of Physiology - Cell Physiology*. 2014;307(8):C684-C98.
4. West JD, Austin ED, Gaskill C, Marriott S, Baskir R, Bilousova G, Jean J-C, Hemnes AR, Menon S, Bloodworth NC, et al. Identification of a common Wnt-associated genetic signature across multiple cell types in pulmonary arterial hypertension. *American Journal of Physiology - Cell Physiology*. 2014;307(5):C415-C30.
5. Martin J, Helm K, Ruegg P, Varella-Garcia M, Burnham E, and Majka S. Adult lung side population cells have mesenchymal stem cell potential. *Cytotherapy*. 2008;10(2):140-51.
6. Summer R, Fitzsimmons K, Dwyer D, Murphy J, and Fine A. Isolation of an Adult Mouse Lung Mesenchymal Progenitor Cell Population. *Am J Respir Cell Mol Biol*. 2007;37(2):152-9.
7. Watkins DN, Berman DM, Burkholder SG, Wang B, Beachy PA, and Baylin SB. Hedgehog signalling within airway epithelial progenitors and in small-cell lung cancer. *Nature*. 2003;422(6929):313-7.
8. Pepicelli CV, Lewis PM, and McMahon AP. Sonic hedgehog regulates branching morphogenesis in the mammalian lung. *Current Biology*. 1998;8(19):1083-6.
9. Liu L, Kugler MC, Loomis CA, Samdani R, Zhao Z, Chen GJ, Brandt JP, Brownell I, Joyner AL, Rom WN, et al. Hedgehog Signaling in Neonatal and Adult Lung. *American Journal of Respiratory Cell and Molecular Biology*. 2013;48(6):703-10.
10. Kramann R, Schneider Rebekka K, DiRocco Derek P, Machado F, Fleig S, Bondzie Philip A, Henderson Joel M, Ebert Benjamin L, and Humphreys Benjamin D. Perivascular Gli1+ Progenitors Are Key Contributors to Injury-Induced Organ Fibrosis. *Cell Stem Cell*. 16(1):51-66.
11. Peng T, Frank DB, Kadzik RS, Morley MP, Rathi KS, Wang T, Zhou S, Cheng L, Lu MM, and Morrissey EE. Hedgehog actively maintains adult lung quiescence and regulates repair and regeneration. *Nature*. 2015;526(7574):578-82.
12. Birbrair A, Zhang T, Files D, Mannava S, Smith T, Wang Z-M, Messi M, Mintz A, and Delbono O. Type-1 pericytes accumulate after tissue injury and produce collagen in an organ-dependent manner. *Stem Cell Research & Therapy*. 2014;5(6):122.
13. Naiche LA, and Papaioannou VE. Loss of Tbx4 blocks hindlimb development and affects vascularization and fusion of the allantois. *Development*. 2003;130(12):2681.
14. Xie T, Liang J, Liu N, Huan C, Zhang Y, Liu W, Kumar M, Xiao R, DİÇÖÖArmiento J, Metzger D, et al. Transcription factor TBX4 regulates myofibroblast accumulation and lung fibrosis. *The Journal of Clinical Investigation*. 2016;126(8):3063-79.
15. Zhang W, Menke DB, Jiang M, Chen H, Warburton D, Turcatel G, Lu C-H, Xu W, Luo Y, and Shi W. Spatial-temporal targeting of lung-specific mesenchyme by a Tbx4enhancer. *BMC Biology*. 2013;11(1):111.
16. Kumar ME, Bogard PE, Espinoza FH, Menke DB, Kingsley DM, and Krasnow MA. Defining a mesenchymal progenitor niche at single cell resolution. *Science (New York, NY)*. 2014;346(6211):1258810-.

17. Hung C, Linn G, Chow Y-H, Kobayashi A, Mittelsteadt K, Altemeier WA, Gharib SA, Schnapp LM, and Duffield JS. Role of Lung Pericytes and Resident Fibroblasts in the Pathogenesis of Pulmonary Fibrosis. *American Journal of Respiratory and Critical Care Medicine*. 2013;188(7):820-30.
18. Sims-Lucas S, Schaefer C, Bushnell D, Ho J, Logar A, Prochownik E, Gittes G, and Bates CM. Endothelial Progenitors Exist within the Kidney and Lung Mesenchyme. *PLOS ONE*. 2013;8(6):e65993.
19. Sheikh AQ, Misra A, Rosas IO, Adams RH, and Greif DM. Smooth muscle cell progenitors are primed to muscularize in pulmonary hypertension. *Science translational medicine*. 2015;7(308):308ra159-308ra159.
20. Armulik A, Abramsson A, and Betsholtz C. Endothelial/Pericyte Interactions. *Circulation Research*. 2005;97(6):512-23.
21. Hellstrom M, Kalon M, Lindahl P, Abramsson A, and Betsholtz C. Role of PDGF-B and PDGFR-beta in recruitment of vascular smooth muscle cells and pericytes during embryonic blood vessel formation in the mouse. *Development*. 1999;126(14):3047-55.
22. Rock JR, Barkauskas CE, Crouse MJ, Xue Y, Harris JR, Liang J, Noble PW, and Hogan BLM. Multiple stromal populations contribute to pulmonary fibrosis without evidence for epithelial to mesenchymal transition. *Proceedings of the National Academy of Sciences*. 2011;108(52):1475-83.
23. Price MA, Wanshura LEC, Yang J, Carlson J, Xiang B, Li G, Ferrone S, Dudek AZ, Turley EA, and McCarthy JB. CSPG4, a potential therapeutic target, facilitates malignant progression of melanoma. *Pigment cell & melanoma research*. 2011;24(6):1148-57.
24. Guimaraes-Camboa N, Cattaneo P, Sun Y, Moore-Morris T, Gu Y, Dalton ND, Rockenstein E, Masliah E, Peterson KL, Stallcup WB, et al. Pericytes of Multiple Organs Do Not Behave as Mesenchymal Stem Cells In  $\text{---}$ áVivo. *Cell Stem Cell*.
25. Xu J, Nie X, Cai X, Cai C-L, and Xu P-X. Tbx18 is essential for normal development of vasculature network and glomerular mesangium in the mammalian kidney. *Developmental Biology*. 2014;391(1):17-31.
26. Sheikh AQ, Lighthouse JK, and Greif DM. Recapitulation of developing artery muscularization in pulmonary hypertension. *Cell reports*. 2014;6(5):809-17.
27. El Agha E, Moiseenko A, Kheirollahi V, De Langhe S, Crnkovic S, Kwapiszewska G, Kosanovic D, Schwind F, Schermuly RT, Henneke I, et al. Two-Way Conversion between Lipogenic and Myogenic Fibroblastic Phenotypes Marks the Progression and Resolution of Lung Fibrosis. *Cell Stem Cell*. 2016.
28. Schultz CJ, Torres E, Londos C, and Torday JS. Role of adipocyte differentiation-related protein in surfactant phospholipid synthesis by type II cells. *American Journal of Physiology - Lung Cellular and Molecular Physiology*. 2002;283(2):L288.
29. Fatima S, Zhou S, and Sorrentino BP. Abcg2 Expression Marks Tissue-Specific Stem Cells in Multiple Organs in a Mouse Progeny Tracking Model. *STEM CELLS*. 2012;30(2):210-21.
30. Hong K, Lee Y, Lee E, Park S, Han C, Beppu H, Li E, Raizada M, Bloch K, and Oh S. Genetic ablation of the BMPR2 gene in pulmonary endothelium is sufficient to predispose to pulmonary arterial hypertension. *Circulation*. 2008;118(722 - 30).
31. Harada N, Tamai Y, Ishikawa T, Sauer B, Takaku K, Oshima M, and Taketo MM. Intestinal polyposis in mice with a dominant stable mutation of the beta-catenin gene. *Embo J*. 1999;18(21):5931-42.
32. Bryant AJ, Robinson LJ, Moore CS, Blackwell TR, Gladson S, Penner NL, Burman A, McClellan LJ, Polosukhin VV, Tanjore H, et al. Expression of mutant bone morphogenetic protein receptor II worsens pulmonary hypertension secondary to pulmonary fibrosis. *Pulmonary Circulation*. 2015;5(4):681-90.
33. Case D, Irwin D, Ivester C, Harral J, Morris K, Imamura M, Roedersheimer M, Patterson A, Carr M, Hagen M, et al. Mice deficient in galectin-1 exhibit attenuated physiological responses to chronic

- hypoxia-induced pulmonary hypertension. *Am J Physiol Lung Cell Mol Physiol*. 2007;292(1):L154-64.
34. Thurlbeck WM. Measurement of Pulmonary Emphysema. *American Review of Respiratory Disease*. 1967;95(5):752-64.